VAHAB SEIF (ORCID: 0000000257795858)[1]
HOSSEIN PEYMAN (ORCID: 0000000151978007)[1, 2]
HAMIDEH ROSHANFEKR (ORCID: 0000000235935274)[1, 2]
SHOHREH AZIZI (ORCID: 0000-0003-0419-9953)[3, 4]
ITANI GIVEN MADIBA (ORCID: 0000-0002-7091-9202)[3, 4]
LINDA LUNGA SIBALI (ORRCID0000-0003-2968-8390)[5]

EVALUATION OF CONTAMINANTS REMOVAL BY A NANOFILTRATION MEMBRANE MODIFIED WITH POLYMER-ION NANOPARTICLES

Iron nanoparticles coated with ionic choline-chloride liquid were used to improve the hydrophilicity and flow rate through the polyethersulfone (PES) membrane. Choline chloride as a modifier was used to obtain the highest water flux by increasing the hydrophilicity of the PES membrane. Changes in membrane structure and morphology were analyzed using FTIR, contact angle, porosity measurement, BET, TGA, DSC, and SEM images. Membrane clogging was measured in the presence of BSA. To evaluate the removal efficiency, Acid Orange 7 dye was used. Suitable removal conditions were obtained by Design-Expert software using a CCD model at optimum pH 6.7 and temperature of 33.9 °C by the DOE method (removal of 97.6%). Iron/choline chloride nanocomposite increased the PES membrane's hydrophilicity and fluid flow rate. Also, the membrane modified by iron/choline chloride nanocomposite removed the sample contaminant from the fluid environment under optimal conditions.

1. INTRODUCTION

Water is the largest natural and vital resource for life on our planet. About four billion people worldwide have no or little access to clean water. These statistical results

---

[1]Department of Chemistry, Ilam Branch, Islamic Azad University, Ilam, Iran, corresponding author H. Peyman, email address: peymanhossein@gmail.com

[2]Arta Shimi Alborz, Research and Development Center, Tehran, Iran.

[3]UNESCO-UNISA Africa Chair in Nanosciences/Nanotechnology, College of Graduate Studies, University of South Africa, Muckleneuk Ridge, P.O. Box 392, Pretoria, South Africa, corresponding author S. Azizi, email address: Shohrehazizi1379@gmail.com

[4]Nanosciences African Network (NANOAFNET) Materials Research Department, iThemba LABS National Research Foundation, P.O. Box 722, Somerset West 7129, Western Cape Province, South Africa.

[5]Department of Environmental Sciences, College of Agriculture and Environmental Sciences, University of South Africa, P.O. Box 392, Florida, 1710, South Africa.

will increase soon due to the excessive discharge and size of micropollutants and contaminants, including pigments and dyes, into the natural water cycle. Most of these pigments have very low biodegradability and some of them are hazardous to aquatic biological activity. These dyes are toxic and carcinogenic, and their accumulation in biological tissues causes irreversible diseases. Therefore, their rapid removal from aqueous solutions is necessary to maintain a healthy and clean aqueous environment [1].

Various techniques have been used to remove colored compounds from wastewater, such as chemical, biological and physical methods [2]. Membrane methods have been applied in this category since the eighteenth century, and have been of considerable interest since the beginning of the twentieth century [3]. Membrane processes with compressive force are proposed due to the significant reduction of energy compared to other methods. Nowadays, membrane technology is widely used in the water treatment industry due to its low destructive effect on the environment and low maintenance and operating costs; the result of this technology is the absorption of most soluble, suspended, and biological contaminants from water. Membrane processes are physical methods for separating solvents from soluble salts using permeable or semi-permeable membranes. Although the separation method with membranes is newer than other methods such as distillation, adsorption, crystallization, and liquid-liquid extraction but due to its efficiency and ease of use, their significant expansion has been observed [4–8].

The use of membranes for purification or separation has advantages over other methods: this method is energy efficient in terms of no need for phase change. Due to the low thickness of membranes and a high level of separation, this method is very efficient. The module in which the membrane is placed has a small volume. Membrane separation methods are combined with other techniques to increase efficiency. Also, the cost of designing and maintaining membrane systems is lower than other traditional methods. Membranes and membrane modules have several advantages. They can be made in different shapes and sizes, no new material is produced during the separation process, and additives that have environmental problems are not used. Membrane processes can be used for heat-sensitive solutions, especially in the food, pharmaceutical and biological industries, because these processes take place at normal temperatures. Moreover, they allow the separation of particles from very dilute solutions [9].

The pore size in nanofiltration is between 0.01 and 0.001 μm. Because these membranes operate at much lower pressures (in comparison to reverse osmosis membranes) and pass some minerals through, they can be used in cases where high removal of organic matter is required as well as moderate mineral removal. Nanofiltration has created optimal conditions in terms of energy cost, ion repellency, and pore size, among other methods. The membranes used in this process are usually composite membranes, of which the top and bottom layers are made up of different polymeric materials and each layer can be made separately. The membranes used in this method are located between open porous membranes and compact and non-porous membranes. Separation in this

case is based on solubility-diffusion. Applications of this process include water treatment, paint, food, and drug industries, removal of heavy metals from industrial effluents, and in recent years the separation of sugar or concentration of sugar solution [10].

The passage of material across the membrane creates a concentration gradient on the feed side and at the membrane's surface. In this way, the density of molecules held by the membrane increases, which reduces the permeability of the membrane and thus reduces the efficiency of the membrane. Most separation processes involve concentration polarization, but membrane processes are significantly more severely affected by this phenomenon [11]. Following concentration polarization, the retained molecules are deposited or adsorbed on the membrane, forming a layer on the surface of the membrane. Thus, over time, the amount of fluid passage from the membrane shows a significant decrease [12]. Due to the following, the amount of flow is affected when a layer forms on the membrane's surface. Since it is an additional layer of resistance on the surface of the membrane, the flux through the membrane decreases at constant pressure. Therefore, an increase in operating pressure can be created to maintain the flux at a constant value [13]. Input feed characteristics, operating conditions, and membrane properties are parameters determining the formation of a layer on the membrane surface The properties of the membrane surface, the type of charge, and the hydrophilicity or hydrophobicity of the membrane strongly affect membrane fouling. In general, smooth membrane surfaces, low surface load, and high hydrophilicity of the membrane will reduce fouling [14].

Polymeric materials such as polypropylene, Teflon, polyamide, polyimide, and polysulfone are now widely used in the manufacture of membranes. High porosity is one of the essential properties of polymer membranes. They are used to recycle hydrocarbons and gases that enter the atmosphere or burn in the relevant processes, so they can be treasured in reducing environmental pollutants. The high reverse selectivity and permeability of these membranes are significant advantages in applications such as the purification of natural gas, the central part of which is methane, which eliminates the need to strengthen the repressor pressure of the purified gas [15]. For the following reasons, polymer membranes are the focus of current membrane research.

The choice of membrane material in designing a membrane process is the first and most crucial issue. At first glance, all polymers can be used as membrane material but in practice, due to the very different physical and chemical properties, only a limited number of them can be used as initial material for the membrane. Each of these materials is used based on its chemical structure, temperature, ambient pH, solubility of materials, and resistance [15].

One of the most common techniques for making polymer membranes is the phase inversion method in which the polymer solution with controlled phase separation into the polymer-rich phase and the polymer-free phases are converted. The polymer-rich phase solidifies immediately after the separation of the phase, forming the main body of the membrane. Membranes made by this method have an asymmetric structure and

their porosity may be high or low [15]. Polyethersulfone (PES) is among the essential polymeric materials commonly utilized in manufacturing microfiltration, ultrafiltration, and nanofiltration membranes. Polyethersulfone-based polymer membranes have thermal stability, mechanical strength, and good chemical resistance. Such membranes are prepared by the phase inversion method, which results in an asymmetric structure. Polyethersulfone-based membranes are widely used, but they have their drawbacks. One of its main disadvantages depends on the relative hydrophobicity of this polymer. Numerous research shows that membrane fouling is related to its hydrophobic properties. Membrane fouling is a fundamental problem in separation, which increases energy demand, reduces membrane life, and results in unpredictable membrane separation performance. Membrane modification methods compromise hydrophobicity and hydrophilicity at the membrane surface, concentrating hydrophilic materials specifically in the membrane pores, where they positively affect flux and sediment reduction.

Various methods were performed to modify the surface of the polymer membranes: physical, chemical, or bulk modification. PES membranes can be modified in different ways due to increased hydrophilicity. Physical or chemical membrane modification processes produce more hydrophilic surfaces after membrane formation. Such processes include the sulfonation resulting in the bonding of carboxylic groups to polyethersulfone [16]. One of the best and most widely used methods of modifying polymer membranes is using nanostructured modifiers, most often iron oxide nanoparticles because of their excellent properties. Two main types of iron oxide nanoparticles are magnetite (Fe_3O_4) and its oxidized type, maghemite (Fe_2O_3). Due to their superparamagnetic properties, they may be used in various fields [17].

One of the problems is the accumulation of iron oxide nanoparticles and their clumping. In addition, polymer membranes have hydrophobic properties that cause the accumulation of contaminants on their surface and low fluid permeability. To solve these problems, other modifiers such as surfactants, etc., are used. In this study, ionic liquids (ILs) are used for the first time.

Since ionic liquids differ from conventional solvents in their special qualities and features, they have emerged as important novel solvents for green chemistry. A new type of IL analog, known as deep active solvent (DES), is used to treat IL deficiencies, including high costs and toxicity. DESs have been shown to have similar properties to IL. Typically, two or three inexpensive and safe components that interact with each other through hydrogen bonds can form DES. Choline chloride (ChCl), a quaternary ammonium salt, is one of the most often used components in DES since it is inexpensive, biodegradable, and non-toxic. In addition, ChCl readily forms a DES with another component containing hydrogen bonds with functional groups (hydrogen bond donors) such as urea, amides, carboxylic acids, and polyols. Over typical ILs, DES-based on ChCl has many advantages, including very straightforward synthesis, no additional purification needed, and the majority of them being biodegradable, biocompatible, and non-

toxic. This is the first time DES generated from ChCl has been used to change magnetic iron nanoparticles and PES membranes, according to earlier work [18].

In optimizing the conditions of an experiment, optimizing each effective parameter alone (one at a time) is used in previous studies. Many experiments caused increasing costs, and also method does not have a high value due to not considering the effect of parameters on each other. Experimental design, often known as DOE (design of experiment) is a modern test design technique that uses a principled approach to comprehend how reaction and product parameters affect response variables like processing, physical characteristics, or product performance. This tool is comparable to any instrument, apparatus, or technique that facilitates experimental study. DOE is a mathematical tool used to establish the significance of particular product or processing variables and control them to improve system performance while maximizing characteristics, in contrast to quality mechanical or process tools. The DOE analyzes the data using statistical techniques to forecast how the product property will behave under all conceivable circumstances within the range chosen for the test design. The interaction between several process and product variables is established in addition to knowing how a specific variable influences product performance. Using experimental limitations, particular laboratory settings, and mathematical analysis to anticipate the response at any point in the experimental range, experimental design is a technique or process of acquiring the necessary information by doing a minimum number of tests. DOE is used to identify the variables and interactions that are crucial in causing the measurable effect and to identify the variables and interactions that are irrelevant and do not affect a specific product characteristic or processing condition. By giving practical concepts regarding properties and reactions, DOE saves time and money. The best time to use DOE when producing a new product or process is to optimize the existing product or process, while if there is more than one variable, technical problems are solved using this method.

The choice of test design method depends on the purpose of the experiment and the number of variables. Experimental design methods are divided into the following types based on the intended objectives: comparative objective, screening, regression design, and response surface method. Response surface methods or RMS (response surface method) ability to estimate quadratic effects and interaction between provides factors and thus the local form of the response surface is easily accessible and checked. RMS design is used to find the optimal point, troubleshoot problems and weaknesses, and create a more substantial and robust process against uncontrollable factors.

In this research, Design-Expert software has been used to optimize the conditions of contaminant removal and response level method [19]. The phase inversion method was used to synthesize the polyethersulfone nanofiltration membrane. Hydrophobicity and repellency of the membrane were improved by iron oxide nanoparticles and ionic chloride ion liquid.

2. MATERIALS AND METHODS

Materials and devices. All materials used in this study were provided with very high purity and were used without preliminary purification. For membrane synthesis, poly-ethersulfone (PES) (BASF, Germany) was used as the base polymer, *N,N*-dimethyl-acetamide (DMAc) (Merck, Germany) as the solvent, and polyethylene glycol (PEG) 400 (Merck, Germany) as the pore maker. $FeCl_3 \cdot 6H_2O$ and $FeCl_2 \cdot 9H_2O$ (Merck, Germany) were used to synthesize iron oxide nanoparticles. The ionic liquid was synthe-sized using choline chloride, urea, and ethanol (Merck, Germany). To adjust pH, hydro-chloric acid, and sodium chloride (Merck, Germany) were used. Acid Orange 7 dye (Sigma Aldrich CAS No. 633965) was used as a sample contaminant in removal exper-iments. Bovine serum albumin (BSA) as the model protein was purchased from Sigma Aldrich. All solutions applied in this study were made with deionized water.

The specially designed and constructed permeation system used in this study ena-bled the testing of the synthesized membranes with a specific diameter of 5 cm. The absorbance of the solutions before and after passing through the membrane was rec-orded using a Lambda 25 Perkin Elmer spectrophotometer at a wavelength of 365 nm. The ultrasonic device of the Alma Sonic P6OH model was used to homogenize the pol-ymer and nanoparticle solutions. Memert oven model UN400 was used to dry the poly-mer and membrane, and pH-meter model GP-353 was used to adjust the pH of the so-lutions. To check the functional groups and correctness of the ionic liquid and modified membrane synthesis, the FTIR technique was used using a Perkin Elmer L160000A device. Nitrogen adsorption/desorption isotherms were used to investigate Brunauer –Emmett–Teller (BET) and Barrett–Joyner–Halenda (BJH) surface isotherms to deter-mine s specific surface area, mean pore size, and pore size distribution (JWGB JW-BK132F). A thermogravimetric analysis (TGA) and differential scanning calorim-etry (DSC) were used to investigate the thermal behavior of non-modified and modified membranes (Perkinelmer STA6000). The hydrophilicity or hydrophobicity of the sur-face of the fabricated membranes was determined by contact angle measurements (ZAM104).

Synthesis of iron nanoparticles. 2.5 g of $FeCl_3 \cdot 6H_2O$ and 3.825 g of $FeCl_2$ was dis-solved in 25 cm³ of distilled water. Then 0.85 cm³ of concentrated HCl was added. The homogeneous mixture was sonicated for 10 min and then 25 cm³ of NaOH 1.5 M solution under intense shaking was added. The solution was centrifuged for 30 min at 4000 rpm. The precipitate was washed with 1000 cm³ of distilled water and sonicated (three repetitive steps). The resulting precipitate was washed with 500 cm³ of 0.01 M HCl, and the precipi-tates adhering to the test vessel were removed [20].

Preparation of iron/choline chloride (FeChCl) composite. 1 g of choline chloride with 2 g of urea were mixed and heated at 100 °C to form a homogeneous liquid and then

allowed to reach room temperature. 1 cm^3 of the ionic solvent in 3 cm^3 of ethanol was dissolved, then 0.2 g of iron nanoparticles was added to 2 cm^3 of ionic liquid–ethanol solution and sonicated for 30 min. After this time, the remaining 1 cm^3 of ethanol solution and the ionic solvent were added and sonicated for 1 h. After sonication, the solution was rested for 24 h, and nanoparticles were separated, washed once with ethanol, and placed at 80 °C to dry [18].

Membrane preparation (18 wt. % PES). Polyethersulfone was prepared as a polymer to make the substrate, PEG as pore maker solvent, and DMAc as a polymer solvent. The phase inversion method was used to fabricate the substrate membranes. The base solution contained: 0.9 g of PES as a base polymer (placed in an oven at 60 °C for 8 h before use to remove moisture), which was slowly added to the solvent, 4 cm^3 of DMAc that was added in two steps, and 0.1 cm^3 of PEG, which was added at the end. The final mixture was mixed using a shaker for 8 h to acquire a homogeneous solution. The prepared solution was then placed overnight in a dark medium and subjected to ultrasonic waves for 15 min (for bubble removal).

A certain amount of the prepared casting solution was applied evenly on a clean glass plate and a film of the desired thickness was cast with the use of a home-made applicator. The cast film was exposed to air for 30 s and then submerged for 2 min in a deionized water bath to initiate the phase inversion process. The cast film was coagulated and the membrane was separated from the glass plate. As the interaction between solvent and non-solvent, the solubility of the solvent in the polymer decreases, and the phase separation becomes faster. This step is the phase inversion, which changes from single-phase to two-phase, polymer-rich, and polymer-free. To ensure the complete removal of the solvent from the membrane structure and final formation, the membrane was immersed in distilled water for 24 h (Table 1). All membrane casting steps were performed at an ambient temperature.

Membranes modified with FeChCl. Half of the required volume of DMAc (4.252 cm^3) was added to the reaction vessel, then the synthesized nanocomposite was added (2.5 mg) and the mixture was subjected to ultrasonication for 1 h. After proper homogenization the vessel was placed on the shaker. At the same time, PES (0.9 g) and the remaining volume of DMAc were added to the vessel. Finally, PEG (88 μl) was added and the mixture was left for 8 h to obtain homogenous mixture.

Properties of membranes. To find membrane permeability, each membrane was placed in a specific location in the permeation system. Then the device was turned on, and the pressure was adjusted to the desired value using the built-in screw. The inlet hose was placed in the tested solution (distilled water or dye solution). The outlet hose was placed in another container equipped with permeation hose, which was inserted in a graduated cylinder.

The permeability system was pressurized to 0.5 MPa for 30 min after the membrane was installed to measure the pure flux. water Pure water permeated through the membrane until a steady state was reached. The permeability of the distilled water was then tested under the pressure of 0.3 MPa. The pure water flux J, dm^3/(m^2·h) or kg/(m^2·h), was calculated using equation

$$J = \frac{V}{At} \tag{1}$$

where V stands for the volume (or mass) of permeating water, dm^3 or kg, A is the membrane surface area, m^2, and t is the time, h. Flux is a crucial parameter for measuring membrane performance. The higher the flux, the higher the filtration ability and the lower operation cost is.

To calculate the membrane porosity ε, wet membranes were weighted and then placed in an oven for 48 h. The dried membrane porosity was calculated using equation

$$\varepsilon = \frac{W_1 - W_2}{Ald_W} \tag{2}$$

where W_1 and W_2 are the weights of the wet and dry membrane, g, respectively, l is the thickness of the membrane, μm, and d_w is the density of water, g/cm^3.

The membrane hydraulic resistance r, m^2/kg, was calculated according to

$$r = \frac{\Delta p}{\mu J} \tag{3}$$

where Δp is the pressure exerted on the membrane surface, Pa, μ is the viscosity of water, Pa·s, and J is the critical flux of the membrane, kg/(m^2·s). The larger the membrane surface and smaller the amount of fluid passing through the membrane surface, the more excellent the membrane resistance is.

Membrane fouling test. The fouling of the membrane was studied by passing a bovine protein (BSA) solution (1 g/dm^3) through the membrane [21]. The membrane was stabilized with distilled water under 0.5 MPa for 30 min and then the water flux under 0.3 MPa was monitored for 1 h (J_{W_1}). Then the NF of the BSA solution was performed until the membrane became clogged (under 0.3 MPa) and the permeate flux (J_p) was monitored for 1 h. In the next step, the membrane was rinsed with distilled water (under shaking), and the pure water flux, J_{W_2}, was measured (under 0.3 MPa).

To evaluate the membrane susceptibility to fouling, the flux recovery ratio (*FRR*), %, was calculated

$$FRR = \frac{J_{W_2}}{J_{W_1}} \times 100\% \tag{4}$$

where J_{W1} and J_{W2} are the pure water fluxes before and after passing the BSA solution, respectively.

Several parameters were defined to describe the anti-fouling properties of the prepared membranes. They are as follows:

The flux reduction due to BSA solution passing through the membrane, R_t, %

$$R_t = \left(1 - \frac{J_p}{J_{W_1}}\right) \times 100\% \tag{5}$$

The flux reduction due to BSA deposition on the membrane surface R_r, %

$$R_r = \frac{J_{W_2} - J_p}{J_{W_1}} \times 100\% \tag{6}$$

The degree of irreversible fouling R_{ir}, %

$$R_{ir} = \frac{J_{W_1} - J_{W_2}}{J_{W_1}} \times 100\% \tag{7}$$

The Guerou–Elford–Ferry equation used to determine the average radius of membrane pores r_m, m:

$$r_m = \left(\frac{8\mu l Q (2.9 - 1.78\varepsilon)}{\varepsilon A \Delta P}\right)^{1/2} \tag{8}$$

where μ denotes water viscosity ($9.8 \cdot 10^{-4}$ Pa·s), l is the membrane thickness, m, Q the volume of water collected per unit of time, m^3/s, ε the membrane porosity, ΔP the operational pressure, Pa.

Parameters affecting the removal of Acid Orange 7. To select the optimal conditions for the removal of Acid Orange 7, pH and temperature as affecting parameters were selected. The selected parameters were examined by the Design-Expert software, DOE (version 11.0.3.0.). The response surface study method, central composite design (CCD) model, and quadratic model were examined according to Table 1. In this design, two levels of response were considered. The temperature range of 25–45 °C was selected for temperature and the range of 3–9 for pH. Low and high levels of these variables were

considered. By applying six repetitions in the central value, the software designed 13 experiments according to Table 1. In each experiment, the amount of dye removed was considered the answer.

<div align="right">T a b l e 1</div>

<div align="center">Performance conditions designed by DOE</div>

Test number	1	2	3	4	5	6	7	8	9	10	11	12	13
pH	3	9	3	9	1	12				6			
Temperature, °C	25		45		35		15	55		35			

The contaminant used in this study was dye – 7.5 μM Acid Orange solution. The NF process was performed to evaluate the dye removal efficiency R, %

$$R = \frac{1 - A_2}{A_1} \times 100\%$$

(9)

where A_1 is the absorbance of the dye solution in the feed and A_2 is the absorbance of permeate. R is the removal efficiency of Acid Orange 7.

3. RESULTS AND DISCUSSION

3.1. FOURIER TRANSFORM INFRARED SPECTROMETRY (FTIR) ANALYSIS

The FTIR results for FeChCls, non-modified membranes, and FeChCl-modified membranes are shown in Fig. 1. Figure 1a shows the FeChCl spectrum. The peak corresponding to Fe–O vibration appears at 559 cm^{-1}. For the ChCl spectrum, a broad band between 3438 cm^{-1} and 3341 cm^{-1} is assigned to O–H mode of alcohols, and the peaks at 3027 cm^{-1} and 2925 cm^{-1} correspond to the CH$_2$ group. Fe-DES, a peak at 1153 cm^{-1}, corresponded to the C–N tensile vibration, indicating a successful synthesis and modification of FeChCl nanocomposites. The peak at 1454 cm^{-1} is assigned to the tensile vibration of choline chloride in DES. Also, vibrations around 3438, 1667, and 1616 cm^{-1} correspond to stretching, bending, and vibration changes of the O–H group [21]. Figure 1b corresponds to the spectrum of pure polyethersulfone. A benzene ring, an ether bond, and a sulfonic structure can be identified in the PES spectrum. A tensile vibration is at 1156 cm^{-1}. The peaks corresponding to stretching vibrations of the C–H bonds in the benzene ring are located at 3026, 2980, and 2925 cm^{-1}. The peaks at 1638, 1487, and 1403 cm^{-1} may be assigned to the appearance of the aromatic structure. The vibration at 1102 cm^{-1} belongs to the C–O group. The appearance of a broad peak in the 3452 cm^{-1} region is related to the O–H bond in the SO$_3$H group. Characteristic peaks located at 1318 and 1242 cm^{-1}

correspond to the C–O–C tensile vibrations. The peaks in the range of 700–1200 cm^{-1} are also related to the tensile vibration of S–O of the sulfone group.
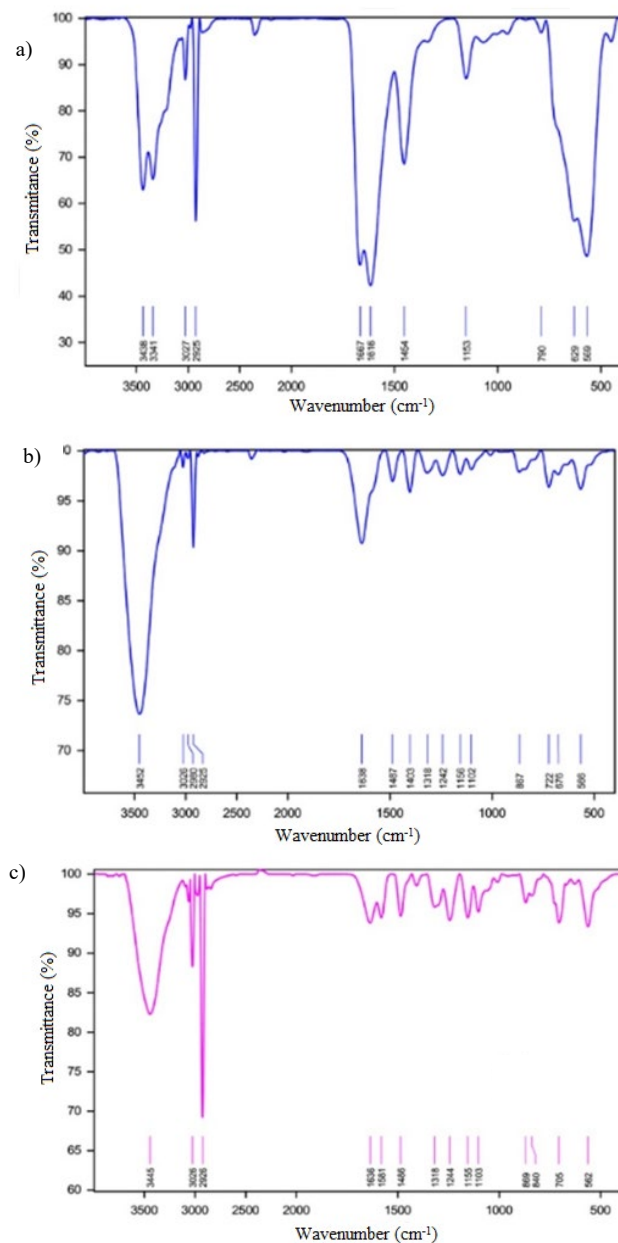
Fig. 1. FTIR spectrum of FeChCl (a), non-modified membrane (b), and FeChCl-modified membrane (c)

Figure 1c shows FTIR spectrum of a membrane modified with a FeChCl nanocomposite. The peak at 2926 cm^{-1} is stronger and more intense than that for the non-modified membrane, and the peak at 1155 cm^{-1}, which is related to Fe–DES, indicates the presence of nanocomposites on the surface of the polyethersulfone film [21].

3.2. BET ANALYSIS

The BET isotherms are given in Fig. 2. The specific surface area in the non-modified PES membrane and PES membrane modified with FeChCl was 23.533 and 16.863 m^2/g, respectively. These results show that the specific surface area is reduced in the modified membrane. The pore volumes in the non-modified PES membrane and PES membrane modified with FeChCl were 0.1966 and 0.1269 cm^3/g, respectively.
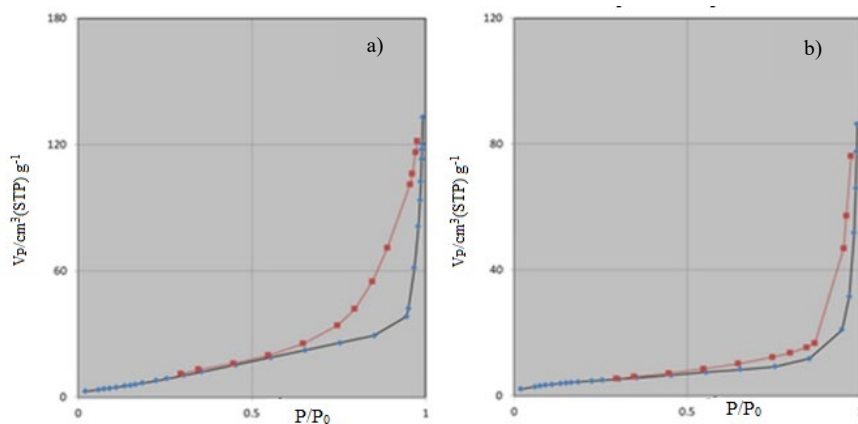
Fig. 2. BET isotherms for non-modified membrane (a) and FeChCl modified membrane (b); P/P_0 is relative pressure, V_p the volume of absorbed (desorbed) gas
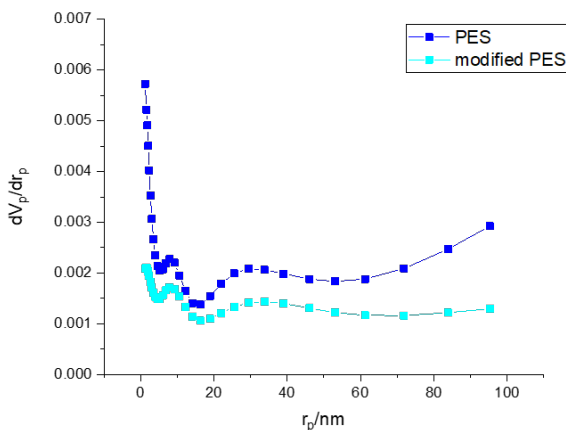
Fig. 3. Volume changes of ratio in dependence of pore radius

These results showed a decrease in the volume of pores after membrane modification. Also, the mean pore diameters of the non-modified PES membrane and PES membrane modified with FeChCl were 3.3423 and 3.0089 nm, respectively, indicating a decrease in pore diameters after membrane modification.

The non-modified membrane diagram shows a larger number of pores for adsorption, indicating a higher specific surface area than the modified membrane (Fig. 3). Therefore, there was more negligible hysteresis than the modified membrane's adsorption. The Langmuir isotherms of the non-modified membrane show higher adsorption than that of the modified membrane. Volume changes relative to the radius of particle pores were determined for both the non-modified and modified membranes. The specific surface areas of the non-modified and modified membranes obtained by the BJH analysis were 25.62 and 14.523 m^2/g, respectively [22].

3.3. SCANNING ELECTRON MICROSCOPY (SEM) AND ENERGY DISPERSIVE X-RAY (EDX) RESULTS

Figure 4 shows the cross-sections of the non-modified membrane and the membrane modified with FeChCl. The membranes have an asymmetric structure with a dense top layer and a porous substrate. Due to the shape, the structure of the non-modified (pure) membrane is closer to the spongy state, and the top layer (separator) is thicker than in other membranes.
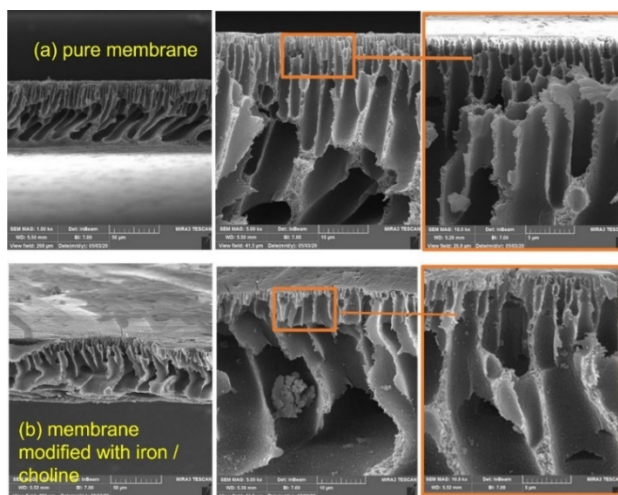
Fig. 4. SEM images related to non-modified (pure) membrane (a)
and membrane modified with iron/choline chloride nanocomposite (b)

Such a structure leads to a lower flow rate than for the unmodified membrane. The structure of the membrane modified by adding 0.5 wt. % of the nanocomposite changed

compared to the structure of the non-modified membrane. The membrane had a lower thickness of the separating layer and a higher substrate thickness. The membrane structure was expanded, and the porosity in the substrate increased. The pores in the separating layer were also larger than in the non-modified membrane. The reason for the formation of such a structure was that the affinity between water and nanomaterial is higher than that of polyethersulfone. Thus the increased rate of water penetration into the forming membrane and the rate of solvent penetration from the membrane to water led to instantaneous phase separation and formation of finger-like pores [23].
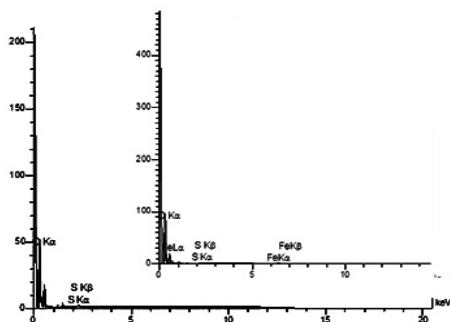
Fig. 5. EDX spectra of the non-modified membrane (lower)
and the FeChCl-modified membrane (upper)

EDX elemental analysis identifies the elements in the composition and confirms the synthesis. Figure 5 shows the EDX spectrum of the non-modified membrane and membrane modified with FeChCl. The figure shows the presence of nanomaterial in the modified membrane.

3.4. THERMAL ANALYSIS

3.4.1. THERMOGRAVIMETRIC ANALYSIS (TGA)

The results of TGA are shown in Fig. 6. The diagram can be divided into three parts: in the range of 0–100 °C the weight loss is due to the evaporation of water molecules and solvent. There was a significant decomposition of the organic skeleton at 300–500 °C but a drastic collapse of the organic skeleton was observed from 500 to 700 °C. The nanocomposite increases the stability of the polymer judging from the mass change from 50.54 to 47.15%. These results are due to the excellent interaction between the polymer and the nanocomposite and the thermal stability of the FeChCl. As the temperature increases and the polymer undergoes thermal degradation, a breakage or slope reduction is observed in the membrane containing the nanocomposite in the temperature range of 540–560 °C. At this stage, the organic part of the nanocomposite decays, and after this

decay, visible weight loss occurs. There is no significant change in sample weight with increasing temperature to 100 °C. The partial weight loss of the non-modified membrane starts from 100 °C, and a significant weight loss of the non-modified membrane starts from 400 °C, indicating the good thermal stability of the PES membrane. The interaction between the nanocomposite and PES increased the strength of the polymer chain, leading to an increase in the energy of the polymer chain decomposition. The degradation temperatures of non-modified membranes and nanocomposite-modified membranes are 400 and 450 °C, respectively, indicating the higher thermal stability of nanocomposite--modified membranes. From this difference, it can be concluded that the addition of nanocomposites to the membrane polymer increases the thermal stability of the membrane [24].
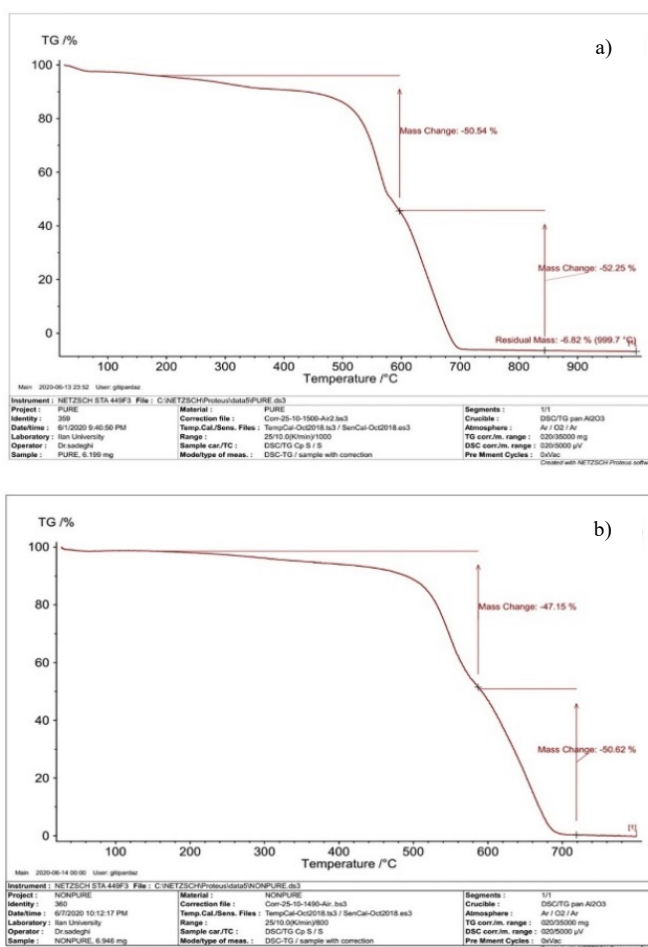
Fig. 6. TGA diagrams for non-modified membrane (a)
and FeChCl-modified membrane (b)

3.4.2. DIFFERENTIAL SCANNING COLORIMETRY (DSC) ANALYSIS

Differential scanning calorimetry (DSC) enables one to find the glass transition temperature (T_g), melting point (T_m), and crystallization temperature (T_c) of polymers, polymer blends, and polymer composites. DSC provides valuable information about the hardness and flexibility of polymer chains and determines the hardening of polymer chains after the addition of nanoparticles. It is also evident that T_g is an essential criterion for component compatibility. Thus, for a thoroughly blended polymer blend, the transfer temperature of a single glass is obtained, while for a non-reversible polymer blend, more than one T_g is obtained. The DSC thermograms of non-modified membrane and membrane modified with FeChCl are shown in Fig. 7.
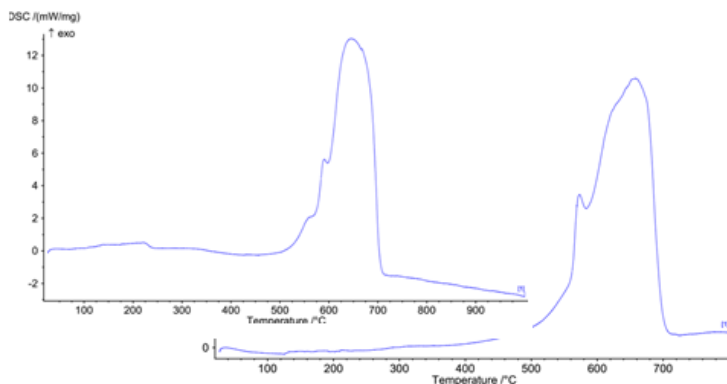
Fig. 7. DSC test results for a non-modified membrane (upper)
and FeChCl-modified membrane (lower)

The membranes had a characteristic glass transfer temperature. Non-modified membranes and modified membranes have peak temperatures of 640 and 680 °C. From these results, it can be found that the addition of nanocomposites to the membrane matrix created excellent flexibility between the polymer and the nanocomposite and increased the heat capacity [21].

3.5. CONTACT ANGLE

The contact angles of the surface of non-modified PES and membranes modified with FeChCl nanocomposites are given in Table 2. The contact angle decreases with increasing nanocomposite content in the membrane structure. It is known that the lower the contact angle of the membrane, the more hydrophilic the membrane and the higher the contact angle the more hydrophobic the membrane is. According to the values reported in Table 2, increasing the amount of FeChCl in the membrane structure decreased the contact angle; this means that the increase in the nanocomposite makes the surface of the membrane hydrophilic. The lowest reported value for the contact angle is for the

modified membrane with 0.5 wt. % of the FeChCl. According to Figs. 8 and 9, the contact angles of the membranes decreased with an increasing weight percentage of FeChCl from 102.3° for non-modified membrane to 57.9° in modified membrane with 0.5 wt. % of FeChCl; this indicates an increase in the hydrophilicity of the membranes [25].

T a b l e 2

Contact angle for PES membranes with various nanocomposite contents

Nanocomposite content, %	0	0.05	0.1	0.2	0.5	0.8
Contact angle, deg	102	95	81.5	73	58	61.5
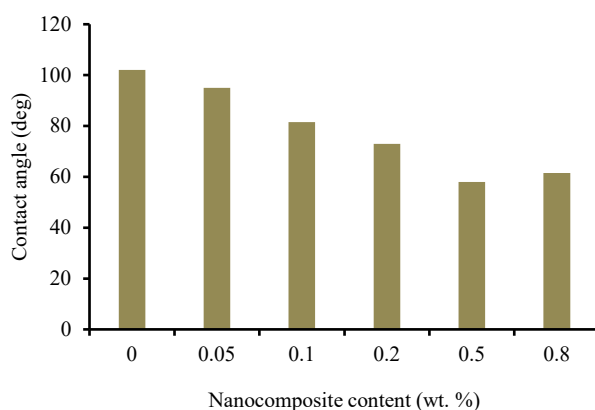
Fig. 8. Contact angles of non-modified and membranes modified with FeChCl
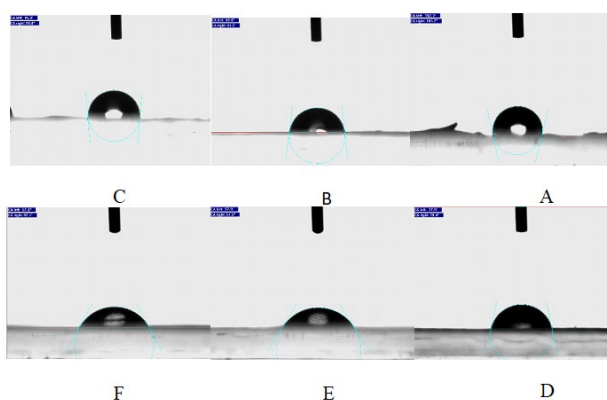
Fig. 9. Contact angles for non-modified membrane, and membranes modified with 0.05, 0.1, 0.2, 0.5, and 0.8 wt. % of FeChCl (A–F, respectively)

3.6. MEMBRANE PROPERTIES

3.6.1. PERMEABILITY

Figure 10 shows the results of pure water and BSA flux tests. The modified membrane with a certain percentage of FeChCl (0.5 wt. %) had the highest value of pure water flux. Water permeability and membrane hydrophilicity were improved. When nanocomposite content amounted to 0.5 wt. % in the membrane matrix the water flux increased by 31% (in comparison to a non-modified membrane). Such a membrane had a maximum water flux of 97 $dm^3/(m^2 \cdot h)$). However, a decrease in water flux was observed at the increased FeChCl content. It can be due to the tendency of accumulation of mineral nanoparticles. However, blockage of membrane surface pores can result from increased nanocomposite content and increased viscosity of the casting solution. A contrasting relationship between the higher viscosity of the casting solution and reduced porosity can significantly reduce the permeability of the PES-modified membranes.
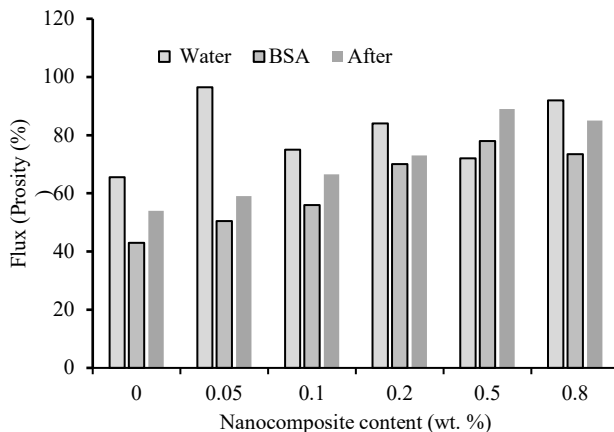
Fig. 10. Flux versus contents of FeChCl in the casting solution
for BSA filtration and pure water before and after NF of BSA solution

3.6.2. FOULING AND MEMBRANE REJECTION

Various problems such as reduced efficiency and increased maintenance costs result from membrane fouling. The consequence of membrane fouling is a reduction in permeate flux. Therefore, most research focused on membrane modification. In the present study, BSA solution of 1 g/dm^3 was used as a common substance to investigate the fouling phenomenon. During pure water permeation after the BSA solution passage, a decrease in membrane permeability was observed (in comparison to pure water flux before NF of BSA solution). The BSA flux for a non-modified membrane was 43 $dm^3/(m^2 \cdot h)$, while for the optimum content of nanocomposite, the flux was 79 $dm^3/(m^2 \cdot h)$ (Fig. 10). It is clear that

the positive effect of FeChCl hydrophilic nanocomposites is significant. Due to the presence of FeChCls in the membrane structure, the permeability of PES membranes and their anti-fouling properties were improved. To obtain an overview of the permeability of the prepared membranes, a comprehensive BSA filtration test and pure water flux (before and after BSA treatment) were performed. As expected, the membrane containing 0.5 wt. % of FeChCl performed best in water flux filtration tests. Due to the good anti-fouling properties of this membrane, the membrane flux after BSA filtration was better than for other membranes. In addition, other membranes exhibited a noticeable decrease in pure water flux in the third stage (after BSA treatment) compared to the first stage. The apparent reduction trend was mainly related to concentration polarization as a result of protein accumulation near the membrane surface. In addition, the FeChCl, with different ratios in the casting solution increased the BSA existence on membrane surface due to electrostatic forces.
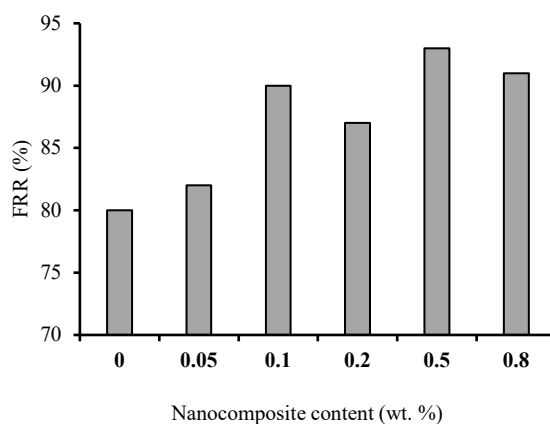
Fig. 11. Flux recovery ratio (*FRR*) for non-modified and modified membranes
versus the contents of FeChCl in the casting solution

The *FRR* parameter was determined to investigate further the fouling phenomenon for non-modified and nanocomposite-modified membranes. Figure 11 shows that by using a specific amount of nanocomposite in the casting solution, it is possible to improve the *FRR* parameter. The maximum and minimum *FRR* values were 92.30 and 80.30% for the modified membrane with 0.5 wt. % of FeChCl content and for the non--modified membrane, respectively. According to the obtained results and previous research, the main reason for the superior anti-fouling performance of the nanocomposite-modified membrane could be its higher hydrophilicity. Membrane hydrophilicity is a controlling factor for adsorption properties, and a more hydrophilic surface should reduce membrane deposition due to more negligible hydrophobic adsorption. The use of FeChCls in the PES membrane structure increases the hydrophilicity of the mem-

branes. This can be seen from another view. Using hydrophilic additives in the hydrophilic membrane matrix increased the surface roughness. In addition, the shear force on the surface of the modified membrane separated the adsorbed sediments relatively better than in the case of the non-modified membrane. A recent study has shown that the growing trend of membrane-action deposition may result from higher mineral additive contents. More than 0.5 wt. % of the nanoparticles in the membrane structure cause roughness of the membrane surface. For more rough membranes sediments can penetrate or adhere within/to the membrane surface, ultimately reducing the flux recovery. Therefore, nanocomposite aggregation can be the main problem of adding more nanocomposites used in the membrane matrix. It is well established that membranes with increased fluxes are prone to fouling. However, nanocomposite-modified membranes prepared with the optimum amount of FeChCl exhibit both flux-enhancing and anti-fouling properties.

The primary source of sediment deposition on the membrane surface is organic matter adsorption and pore blocking. Total membrane deposition (R_t) consists of reversible deposition (R_r) and irreversible deposition (R_{ir}). Irreversible deposition occurs due to the strong adsorption of sediments on the surface or their fouling in the pores. Reversible deposition is due to poor adsorption of sediments, which can be removed by simple membrane washing. Figure 12 shows the results of the permeation tests and the fouling resistance ratios calculated based on the water flux before NF of the BSA solution, permeate flux for NF of the BSA solution, and after the membrane washing with distilled water. The ratio of irreversible fouling for the membrane modified with FeChCl (0.5 wt. %) was markedly reduced in comparison to the non-modified membrane [25].
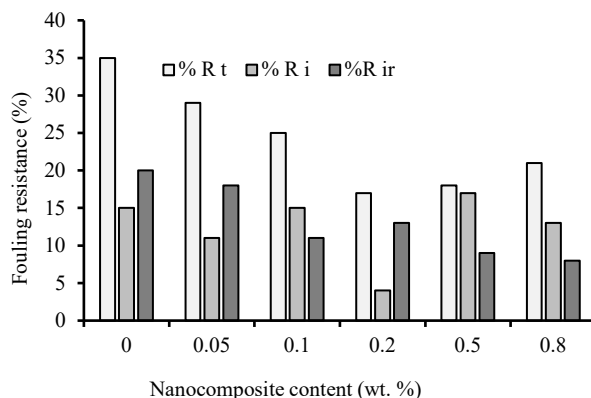
Fig. 12. Fouling resistance ratios for non-modified and modified membranes
versus the contents of FeChCl in the casting solution

3.6.3. MEMBRANE POROSITY

Membrane water content measures hydrophilicity and membrane swelling rate and is related to membrane porosity. The effect of adding FeChCl to the polymer solution on the porosity is shown in Fig. 13. The membrane porosity was reduced by adding nanocomposite at the amount of 0.05 wt. %. Due to the small amount of nanocomposite, little change in the hydrophilicity of the membrane was achieved, and the nanocomposite did not affect the phase separation rate and, consequently, the porosity of the membrane. Porosity was reduced by filling the pores with nanocomposites. As a result, the membrane has less capacity to hold water.
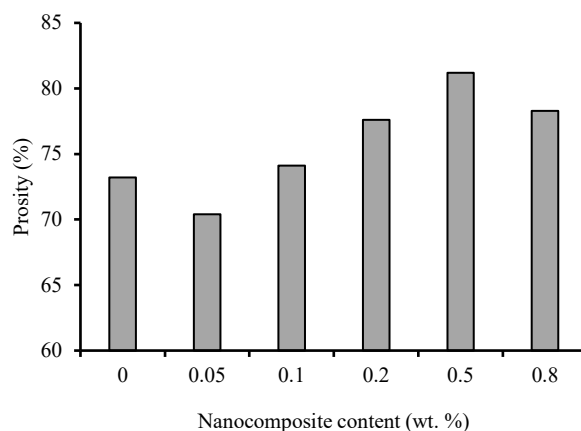
Fig. 13. The effect of different concentrations of nanoparticles on membrane porosity

By increasing the amount of nanocomposite to 0.5 wt. %, the membrane porosity increased. This increase was partly due to the hydrophilic nature of FeChCls and partly due to the enormous growth of pores in the substrate. Because nanocomposites are hydrophilic, they accelerate the removal of solvents from the polymer film and open the membrane structure. The presence of substances with similar non-solvent properties (ion-free water) accelerates the exchange of solvent and non-solvent. On the other hand, the formation of polymer-nanocomposite bonds reduces the polymer interaction and makes the casting film more unstable. Therefore, phase separation occurs faster in the coagulation bath. As a result, the porosity increases, and the membrane can retain more water. At the nanoparticles concentration of 0.8 wt. %, pore blockage with additional amounts of nanocomposite leads to fewer pores, less porosity, and a closer membrane structure. Reduced porosity reduces the membrane permeability [21].

3.7. REMOVAL OF POLLUTANTS

The modified membrane was used to remove the acid dye. Six PES membranes were prepared from casting solutions containing different amounts of polymer. The best

non-modified membrane (of a thickness of 160 µm) was obtained from a polymer solution containing 18 wt. % of PES. By adding FeChCl to the membrane casting solution, the membrane modified with 0.5 wt. % of nanocomposite was selected as the optimal membrane according to SEM images as well as fouling and porosity tests. This optimal membrane was used to remove Acid Orange 7 from aqueous solutions, and the conditions and parameters affecting the dye removal were investigated using the experimental design method. To investigate the effect of two parameters (temperature and pH) on the percentage of dye removal, 5 µM solutions were prepared. The tests were performed according to the data of the Design-Expert software, CCD method at various temperatures, and pH with membrane modified by the addition of 0.5 wt. % of the nanocomposite. The software designed 13 experiments, of which 6 were membrane tests to replicate the central value. The experiments were performed in the required conditions, and the removal percentage was calculated and presented to the software. The results are shown in Table 3.

T a b l e 3

Acid Orange 7 contents before (A_1) and after (A_2) filtration
(0.5 wt. % of nanocomposite)

Test number	Temperature [°C]	pH	A_1	A_2	Removal [%]
1	25	3	0.03391	0.00251	92.59
2		9	0.00462	0.01991	76.8
3	45	3	0.02292	0.01276	44.3
4		9	0.10276	0.02371	77
5	35	1	0.01571	0.01431	9
6		12	0.42194	0.25885	38.6
7	15		0.43477	0.21685	50.1
8	55		0.44697	0.25885	42.1
9			0.01645	0.00469	71.5
10		6	0.04822	0.0064	86.7
11	35		0.44596	0.05106	88.5
12			0.45814	0.04259	90.7
13			0.45831	0.06572	85.6

3.7.1. DYE REMOVAL WITH DESIGN-EXPERT SOFTWARE

Design-Expert software has selected the quadratic model from various models for statistical data (Version 11.0.3.0). The quadratic model is the most appropriate model for this study, as statistical calculations and correlation coefficients show, because, in addition to having the appropriate correlation coefficients, the calculated PRESS amount is also in the most optimal state. Therefore, the cube model for calculations in other parts was chosen. After selecting the model, to investigate the effect of factors affecting the result (temperature and pH on the removal efficiency), statistical parameters of each of these variables were calculated by the Anova method in the quadratic model (Table 4).

Statistical data (Anova)

Source	Sum of squares	df	Mean square	F-value	p-value	
Model	4616.08	5	923.22	365.83	<0.0001	
A–pH	458.94	1	458.94	181.86	<0.0001	
B–temperature	269.04	1	269.04	106.61	<0.0001	significant
AB	479.61	1	479.61	190.05	<0.0001	
A²	2548.31	1	2548.31	1009.78	<0.0001	
B²	1853.63	1	1853.63	734.51	<0.0001	
Residual	15.14	6	2.52			
Lack of fit	4.75	2	2.37	0.9141	0.4710	not significant
Pure error	10.39	4	2.60			
Cor. total	4631.22	11				

In addition to the individual effect of each variable, the degree of correlation between the variables and the effect of power in each have also been investigated. The values of the obtained parameters P and F (Tables 5–7) show that pH and temperature have an independent and correlated effect on the result as is expressed in the equation obtained:

$$Y = 17.95 + 13.42A + 3.63B + 0.36AB - 1.90A^2 - 0.09B^2$$

where A is pH and B temperature. To investigate the dispersion of deletion percentage data from two graphs, normal plot of residuals and residuals versus predicted was used. These curves show that the lower the scatter around the curve line, the minor error and the results are random, and the work error is less (Figs. 14 and 15). The accepted error limit in the calculations is assumed to be 5%, but as seen in the above curves, the data are scattered in the 2% range, indicating a high level of reliability at work and less error.

Fitting the data for the selected model

Source	Sequential p-value	Lack of fit p-value	Adjusted R²	Predicted R²	Comment
Linear	0.7231	<0.0001	–0.1373	–1.1018	
2FI	0.3462	<0.0001	–0.1370	–1.5766	
Quadratic	<0.0001	0.4710	0.9940	0.9786	
Source	Sum of squares	df	Mean square	F-value	p-value	suggested
Linear	4298.92	5	859.78	330.94	<0.0001	
2FI	3819.31	4	954.83	367.52	<0.0001	
Quadratic	4.75	2	2.37	0.9141	0.4710	suggested
Cubic	0.0000	0				aliased
Pure Error	10.39	4	2.60			

Specifications of the Design-Expert software used

File version	11.0.3. 0		
Study type	response surface	subtype	randomized
Design type	central composite	runs	13
Design model	quadratic	blocks	no blocks
Build time, ms	1.0000		

Deviations calculated and proposed by Design-Expert software

Source	Standard deviation	R^2	Adjusted R^2	Predicted R^2	PRESS	
Linear	21.88	0.0695	−0.1373	−1.1018	9734.05	
2FI	21.88	0.1731	−0.1370	−1.5766	11933.02	
Quadratic	1.59	0.9967	0.9940	0.9786	99.02	suggested
Cubic	1.61	0.9978	0.9938		*	aliased
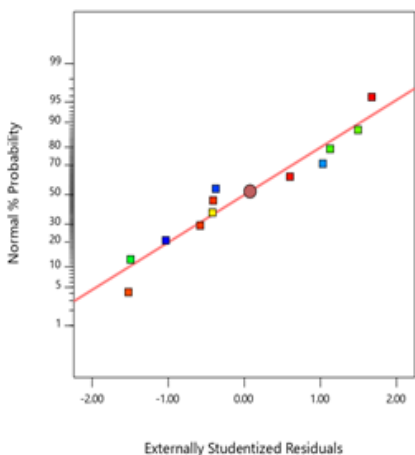
Fig. 14. Scattering degree
for dye removal efficiency
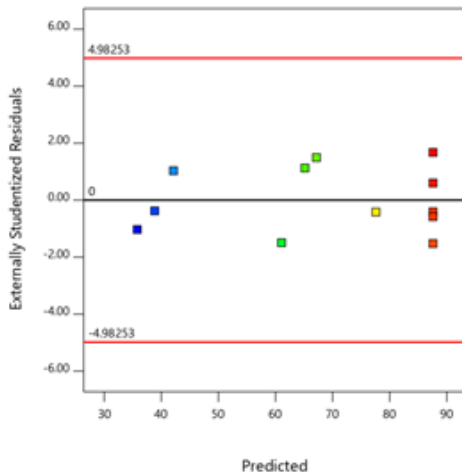
Fig. 15. Dispersion of deletion percentage data

3.7.2. ERROR THAT OCCURRED DURING CHANGING pH AND TEMPERATURE

To evaluate each variable error, the distribution of the results concerning each variable was calculated. According to Figs. 16 and 17, the error in changing the pH and temperature is standard. In this case, the maximum error and scatter observed is 2%, which is much less than the maximum allowable value (5%), which indicates perfect accuracy in conducting research and low error in test results.
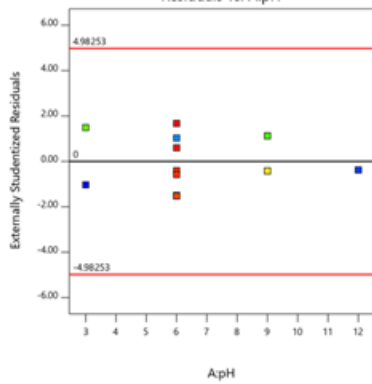
Fig. 16. Error occurred in pH change
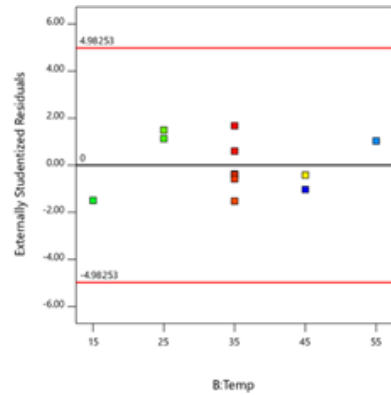
Fig. 17. Error occurred in temperature change

3.7.3. OPTIMAL NF PROCESS CONDITIONS

To obtain the optimal NF process conditions, we use the two-dimensional shape (Fig. 18) and three-dimensional one, not shown here extracted from the Design-Expert software. In severe acidic and alkaline conditions, the removal percentage decreases due to protonation or very high concentrations of hydroxyl groups. The best conditions in terms of pH are around the neutral zone. Changing the temperature will also change the plasticity of the membrane, resulting in ease or difficulty of fluid passage and in the change of the removal rate. The optimum temperature is around 34 °C (Tables 8 and 9). To confirm the optimal conditions of this pH and temperature, removal was performed twice. The obtained average and desired values are close to each other (Table 10).
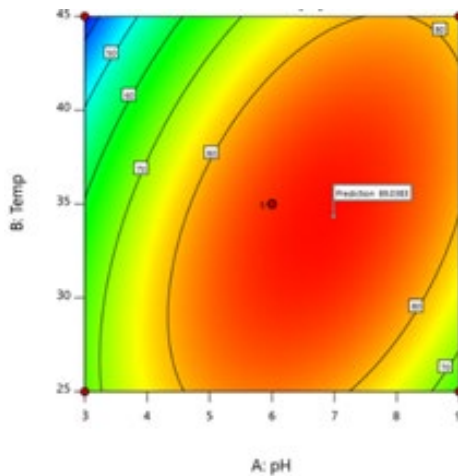
Fig. 18. Dye removal efficiency
in function of temperature and pH

Statistical parameters of the fitted model

Std. dev.	1.59	R^2	0.9967
Mean	68.81	adjusted R^2	0.9940
C. V. %	2.31	predicted R^2	0.9786
		adeq. precision	46.1091

Calculated optimal conditions for dye removal by NF

Factor	Level	Low level	High level	Coding
pH (A)	6.77	3.00	9.00	actual
Temperature (B)	33.92	25.00	45.00	

Values predicted by repeating the answer in optimal conditions

Response	Std. dev.	SE pred.	95% PI low	Data mean	95% PI high
Removal	1.58859	1.32328	85.8737	91.2	92.3496

4. CONCLUSION

In this study, for the first time, ionic liquid chloride ion and iron oxide nanoparticles were used to modify the structure and hydrophilicity of the polyethersulfone nanofiltration membranes. Membrane parameters were investigated by fluid passage and using different decomposition methods. The experimental design method and response level model were used to optimize the parameters affecting contaminant removal statistically. The results showed structural modification, increased hydrophilicity, and increased membrane removal properties under optimal temperature and pH conditions. The maximum removal efficiency of Acid Orange 7 was found to be 97.6% at optimum conditions of pH 6.7 and temperature of 33.9 °C.

REFERENCES

[1] Bansal P., Chaudhary G.R., Mehta S.K., *Comparative study of catalytic activity of ZrO₂ nanoparticles for sonocatalytic and photocatalytic degradation of cationic and anionic dyes*, Chem. Eng. J., 2015, 280, 475–485. DOI: 10.1016/j.cej.2015.06.039.
[2] Zhao C., Deng H., Li Y., Liu Z., *Photodegradation of oxytetracycline in aqueous solution by 5A and 13X loaded with TiO₂ under UV irradiation*, J. Hazard. Mater., 2010, 176, 884–892. DOI: 10.1016 /j.jhazmat.2009.11.119.
[3] Zad Z.R., Davarani S.S.H., Taheri A.R., Bide Y., *Highly selective determination of amitriptyline using Nafion-AuNPs@ branched polyethyleneimine-derived carbon hollow spheres in pharmaceutical drugs and biological fluids*, Biosens. Bioelectron., 2016, 86, 616–622. DOI: 10.1016/j.bios.2016.07.028.

[4] Farmani M.R., Peyman H., Roshanfekr H., *Blue luminescent graphene quantum dot conjugated cysteamine functionalized-gold nanoparticles (GQD-AuNPs) for sensing hazardous dye Erythrosine B*, Spectrochim. Acta, Part A, Mol. Biomol. Spectry, 2020, 229, 117960. DOI: 10.1016/j.saa.2019.117960.

[5] Rahimi F., Roshanfekr H., Peyman H., *Ultra-sensitive electrochemical aptasensor for label-free detection of Aflatoxin B1 in wheat flour sample using factorial design experiments*, Food Chem., 2021, 343, 128436. DOI: 10.1016/j.foodchem.2020.128436.

[6] Gholivand M.B.B., Peyman H., Gholivand K., Roshanfekr H., Taherpour A.A.A., Yaghobi R., *Theoretical and instrumental studies of the competitive interaction between aromatic α-amino-bisphosphonates with DNA using binding probes*, Appl. Biochem. Biotechnol., 2017, 182, 925–943. DOI: 10.1007/s12010-016-2371-6.

[7] Ghasemi J., Peyman H., Niazi A., *Spectrophotometric determination of acidity constants of 4-(2-pyridylazo) resorcinol in various micellar media solutions*, J. Chinese Chem. Soc., 2007, 54, 1093–1097. DOI: 10.1002/jccs.200700156.

[8] Alidadykhoh M., Pyman H., Roshanfekr H., *Application of a new polymer AgCl nanoparticles coated polyethylene terephthalate [PET] as adsorbent for removal and electrochemical determination of methylene blue dye*, Chem. Meth., 2021, 5, 96–106. DOI: 10.22034/chemm.2021.119677.

[9] Bartels C.R., Wilf M., Andes K., Iong J., *Design considerations for wastewater treatment by reverse osmosis*, Water Sci. Technol., 2005, 51, 473–482. DOI: 10.2166/wst.2005.0670.

[10] Wang X.-L., Wang W.-N., Wang D.-X., *Experimental investigation on separation performance of nanofiltration membranes for inorganic electrolyte solution*s, Desalin., 2002, 145, 115–122. DOI: 10.1016 /S0011-9164(02)00395-8.

[11] Strathmann H., *Membranes and membrane separation processes*, [In:] *Ullmann's Encyclopedia of Industrial Chemistry*, Wiley-VCH, 2000. DOI: 10.1002/14356007.a16_187.pub2.

[12] See Toh Y.H., *Green asymmetric molecule manufacture using organic solvent nanofiltration and homogeneous catalyst recycle*, Thesis, Department of Chemistry, Imperial College, London SW7 2BY, UK, 2005.

[13] Stumm W., *Aquatic colloids as chemical reactants: surface structure and reactivity*, Colloids Surf. A: Physicochem. Eng. Asp., 1993, 73, 1–18. DOI: 10.1016/0927-7757(93)80003-W.

[14] Tang C.Y., Fu Q.S., Criddle C.S., Leckie J.O., *Effect of flux (transmembrane pressure) and membrane properties on fouling and rejection of reverse osmosis and nanofiltration membranes treating perfluorooctane sulfonate containing wastewater*, Environ. Sci. Technol., 2007, 41 (6), 2008–2014. DOI: 10.1021 /es062052f.

[15] Naylor T.V. de, *Polymer Membranes: Materials, Structures, and Separation Performanc*e, iSmithers Rapra Publishing, 1996.

[16] Ran F., Li J., Lu Y., Wang L., Nie S., Song H., Zhao L., Sun S., Zhao C., *A simple method to prepare modified polyethersulfone membrane with improved hydrophilic surface by one-pot. The effect of hydrophobic segment length and molecular weight of copolymers*, Mater. Sci. Eng. C., 2014, 37, 68–75. DOI: 10.1016/j.msec.2013.12.037.

[17] Wei Y., Han B., Hu X., Lin Y., Wang X., Deng X., *Synthesis of Fe_3O_4 nanoparticles and their magnetic properties*, Proc. Eng., 2012, 27, 632–637. DOI: 10.1016/j.proeng.2011.12.498.

[18] Huang Y., Wang Y., Pan Q., Wang Y., Ding X., Xu K., Li N., Wen Q., *Magnetic graphene oxide modified with choline chloride-based deep eutectic solvent for the solid-phase extraction of protein*, Anal. Chim. Acta., 2015, 877, 90–99. DOI: 10.1016/j.aca.2015.03.048.

[19] Kirk S.A., Gomory T., Cohen D., *Mad Science. Psychiatric coercion, Diagnosis, and Drugs*, Routledge, 2017.

[20] Abbasi A.R., Akhbari K., Morsali A., *Dense coating of surface mounted CuBTC metal-organic framework nanostructures on silk fibers, prepared by layer-by-layer method under ultrasound irradiation with antibacterial activit*y, Ultrason. Sonochem., 2012, 19, 846–852. DOI: 10.1016/j.ultsonch.2011.11.016.

[21] Vinodhini P.A., Sangeetha K., Thandapani G., Sudha P.N., Jayachandran V., Sukumaran A., *FTIR, XRD and DSC studies of nanochitosan, cellulose acetate, and polyethylene glycol blend ultrafiltration membranes*, Int. J. Biol. Macromol., 2017, 104, 1721–1729. DOI: 10.1016/j.ijbiomac.2017.03.122.

[22] Duan Y.-T., Sangani C.B., Ameta R.K., *Thermal, SEM, AFM, BET and biological analysis of newly synthesized Fe^{2+}/Fe^{3+}-based MOIFs*, J. Mol. Liq., 2019, 295, 111709. DOI: 10.1016/j.molliq.2019.111709.

[23] Kebria M.R.S., Jahanshahi M., Rahimpour A., *SiO_2 modified polyethyleneimine-based nano-filtration membranes for dye removal from aqueous and organic solutions*, Desalin., 2015, 367, 255–264. DOI: 10.1016/j.desal.2015.04.017.

[24] Makhetha T.A., Moutloali R.M., *Antifouling properties of Cu (tpa)@ GO/PES composite membranes and selective dye rejection*, J. Membr. Sci., 2018, 554, 195–210. DOI: 10.1016/j.memsci. 2018.03.003.

[25] Livazovic S., *Ultrafiltration and Nanofiltration Multilayer Membranes Based on Cellulose*, PhD dissertation, King Abdullah University of Science and Technology, Thuwal, Kingdom of Saudi Arabia, 2016.